Spectrum sensing assisted by windowing for fast time-varying channel

Kais Bouallegue, Matthieu Crussière

Spectrum Sensing Assisted by Windowing for Fast Time-varying Channel

Kaïs Bouallegue, Matthieu Crussière

Univ Rennes, INSA Rennes, CNRS, IETR - UMR 6164, Rennes, France.

Abstract

In this paper, we introduce new totally blind spectrum sensing (SS) algorithms, for fast time-varying channel, based on eigenvalue decomposition (EVD) of the covariance matrix of the received signal. The new scheme is based on the sliding window whose the size depends on the coherence time of the channel. First, we evaluate the impact of the mobility on the detection performance. Then, by applying EVD in each window, we focus our study on the maximal estimated largest eigenvalue (MELE). We provide simulation results in order to validate the proposed theoretical expression of the probability density function of the MELE. Finally, simulation results illustrate the performance of the contributions and are compared to other SS methods.

Keywords: Spectrum sensing, time-varying channel, cognitive radio, sliding window.

1. Introduction

This last decade, cognitive radio (CR) systems which are able to sense their radio surroundings, have attracted more and more attention to tackle the scarcity of the frequency spectrum by enabling opportunistic resource utilization. This issue is all the more relevant today when many new technologies, such as the Internet of things (IoT) [1]. Thus, it is relevant to explore the integration of newly emerging technologies with the CR-based IoT systems [2]. In CR networks, one defines two kinds of users, the primary user (PU) who has all the priority on the frequency band and the secondary user (SU) who can opportunistically benefit from some part of the spectrum resource. The SU indeed aims at exploiting the spectrum holes through a dynamic reconfiguration of the radio frequency front-end. In this context,

the SU has thus to be always aware of its environment. This is achieved by applying the so-called cognition loop to identify the available spectrum resource and then as possible at least not interfere with the PU. The decision on the availability or unavailability of the resource is based on the result of the spectrum sensing (SS) step which is the basic building block of any CR system. The first standard defining CR system capabilities is the wireless regional area networks (WRAN) IEEE 802.22 designed for the bands assigned to TV broadcasting. The performance constraints of this standard is to sense the PU, for a signal-to-noise ratio (SNR) around -21 dB, at a probability of detection (P_d) of at least 0.9 and a probability false alarm (P_{fa}) lower than 0.1 [3]. But the CR network can be exploited for other applications:

1. Next generation wireless networks: Cognitive radio is promising technology for the next generation of heterogeneous wireless networks. Cognitive radio will provide intelligent information for both the user equipment and the network equipment provider. A mobile device can observe the state of wireless access networks (transmission quality, speed, delay) and make a decision on the selection of network access.
2. Cyber health services (eHealth services): Different types of wireless technologies are adopted in health services to improve the efficiency of patient care and healthcare management. The concepts of cognitive radio are user in order to allow the multiples wireless medical sensors to choose the best transmission bands to avoid interference and to ensure a better quality of service.
3. Emergency Networks: Public safety and emergency networks use the concepts of cognitive radio to provide reliability and flexibility in wireless communications. In disaster, standard communications infrastructures are not available ; a cognitive radio network may be required to support wireless communication after the disaster.
4. Military networks: The parameters of wireless communication can be dynamically adapted according to time and location as well as the soldier's mission. For example, if certain frequencies are jammed or noisy, cognitive radio devices (transmitters / receivers) can search for alternative access frequency bands for communications.

Recently, many research studies have focused on new blind SS methods using multiple-input multiple-output (MIMO) configuration and exploiting the covariance matrix of the received signal. Some methods track scalar metrics directly computed from the entries of the covariance matrix, such

as the covariance Frobenius norm (CFN) or the covariance absolute value (CAV) [4]. Other classes of methods are rather based on eigenvalue decomposition (EVD) of the covariance matrix, such as the blindly combined energy detection (BCED) [5], the arithmetic-to-geometric mean (AGM) [6], the energy with minimum eigenvalue (EME), maximum-minimum eigenvalue (MME) [7], the unified sensing algorithm (USA) [1], the maximum-eigenvalue-geometric-mean (MEGM) [8], the mean-to-square extreme eigenvalue (MSEE) [9] algorithms and a combined fully blind self adapted two-stage approach [10]. Recent contribution introduces the machine learning, specifically the radial basis function support vector machine (RBF-SVM) to improve the sensing performance [11]. However, all these methods were originally designed for quasi-static channels and are not adapted for the high mobility issue.

To improve the PU detection [12], new contributions proposed beamforming approach such as maximum-to-minimum beam energy [13], maximum-to-mean energy detector [14] and maximum energy beamforming-output-to-input [15]. But these methods consider ray propagation channel.

Recent contributions for time-varying channels essentially are based on applying weights on the covariance matrix of the received signal to adequately smooth the effects of the channel response modifications [16]. As this strategy is sensitive to the correlation between receive antennas, the authors in [17] considered the Ljung-Box (LB) test for CR networks with low-correlated receive antennas. However the detection performance of the LB test decreases in low SNR regions. When the number of antennas is not large enough. The impact of mobility has also been well investigated in [18] for cooperative SS in vehicular networks. The impact of acceleration on the detection performance for energy detection is proposed in [19]. This work is, however, based on energy, whose performance depends on the perfect knowledge of the noise level.

Contrary to the contributions cited above, we propose in this paper to improve the robustness of the SS algorithms based on the EVD strategy for fast-varying channels. To that aim, we define a sliding window (SW) on the observed samples to mitigate the effects of the channel variations onto the EVD-based detection metrics. The concept of sliding window has indeed been used in [20] for SS algorithms considering orthogonal frequency division multiplex (OFDM) system. It is extended and analyzed here for the BCED sensing method. Namely, we first derive the statistical test of the proposed SW-BCED algorithm which turns out to be reliant on the

maximal estimated largest eigenvalue (MELE). We then evaluate and propose an analytical expression of the probability density function of the MELE among all the windows.

The MELE is then applied to the BCED algorithm and comparison results with the original algorithm are provided in order to illustrate the contribution of the windowing in the sensing performance.

2. System model

Let us consider a CR terminal as the SU with $M(M > 1)$ receiving antennas. We assume the following scenario, a fixed PU and a moving SU equipped with a speedometer. We define two hypotheses $\mathcal{H}_0$, when the resource is vacant and $\mathcal{H}_1$, when the PU is present.

We assume a frequency-flat fading and time-selective channel. The source signal from the PU is assumed to be independent and identically distributed (i.i.d.). The received signal vector is expressed as

$$\mathbf{y}(n) = \xi \mathbf{H}(n)\mathbf{x}(n) + \mathbf{b}(n), \quad n = 1, 2, \cdots, N \tag{1}$$

where $\xi = 0$ under $\mathcal{H}_0$, $\xi = 1$ under $\mathcal{H}_1$, N is the number of samples, $\mathbf{y}(n)$ is the received signal, $\mathbf{x}(n)$ is the transmitted signal from the PU, Rayleigh fading channel, noted $\mathbf{H}(n)$, is the spatially-uncorrelated complex matrix of the MIMO channel at instant n

$$\mathbf{b}(n) = [b_1(n), b_2(n), \cdots, b_M(n)]^T \tag{2}$$

is a zero-mean additive white Gaussian noise with variance σ_b^2. Each channel matrix entry $h_{ik}(n), i = 1, ..., M$, $k = 1, ..., \mathrm{K}$, is Rayleigh distributed and time-varying for each MIMO symbol n with M receive antennas and K transmit antennas $(M > K)$. The time variation considered in this paper is the Jake's model. The Jakes' model [21] is widely used to represent the Doppler power spectrum of a mobile radio channel. The autocorrelation function of the channel is given by

$$r_h(\tau) = J_0(2\pi f_d \tau), \tag{3}$$

Notation: Boldface lower letters to denote vectors and boldface capital letters to denote matrices. Superscript $(.)^T$ and $(.)^H$ stand for transpose and Hermitian (complex conjugate transpose) respectively. $Tr(.)$ denotes the trace of a matrix. $\mathbf{I}_u$ denotes the identity matrix of order u.

where $J_0(.)$ is the zero-order Bessel function of the first kind, $f_d = v/\lambda$ is the maximum Doppler frequency, where v is the speed of the SU and λ is the carrier wavelength. Obviously, knowing the frequency carrier to sense, the SU can easily determine the maximum Doppler frequency.

3. Background on Blindly Combined Energy Detector (BCED)

We introduce a well-known eigenvalue-based spectrum sensing detector called BCED [5] which provides good performance in non-cooperative context [13]. First, the covariance matrix of the received signal is defined as

$$\mathbf{R}_y(n) = \mathbf{H}\mathbf{R}_x\mathbf{H}^H + \sigma_b^2\mathbf{I}_M, \tag{4}$$

where

$$\mathbf{R}_y = E[\mathbf{y}(n)\mathbf{y}(n)^H] \tag{5}$$
$$\mathbf{R}_x = E[\mathbf{x}(n)\mathbf{x}(n)^H]. \tag{6}$$

Then, the eigenvalues are extracted from the covariance matrix $\mathbf{R}_y$ and are noted $\ell_1, \ell_2, \cdots, \ell_M$ such that $\ell_1 \geqslant \ell_2 \geqslant \cdots \geqslant \ell_M$. After that, the statistical test is calculated and is expressed as

$$T_{\text{BCED}} = \frac{\ell_1}{\frac{1}{M}Tr(\hat{\mathbf{R}}_{\mathbf{y}})} \underset{\mathcal{H}_1}{\overset{\mathcal{H}_0}{\lessgtr}} \gamma_{\text{BCED}}, \tag{7}$$

where γ_{BCED} is the threshold well investigated in [22] using the random matrix theory.

In pratice, the estimated covariance matrix of the received signal $\hat{\mathbf{R}}_{\mathbf{y}}$ with N samples is given by

$$\hat{\mathbf{R}}_{\mathbf{y}} = \frac{1}{N}\sum_{n=1}^{N}\mathbf{y}(n)\,\mathbf{y}^H(n). \tag{8}$$

In $\mathcal{H}_0$ context, the covariance matrix $\hat{\mathbf{R}}_{\mathbf{y}}$ follows a Wishart complex distribution corresponding to the generalization to multiple dimensions of the chi-squared distribution χ^2. Based on that, the expression of the threshold is given by the probability of false alarm

$$P_{fa} = 1 - F_{\mathrm{TW}}\left(\frac{\gamma_{\mathrm{BCED}} - \mu_{N,M}}{\sigma_{N,M}}\right) + \frac{1}{MN}\left(\frac{\mu_{N,M}}{\sigma_{N,M}}\right)^2 F''_{\mathrm{TW}}\left(\frac{\gamma_{\mathrm{BCED}} - \mu_{N,M}}{\sigma_{N,M}}\right), \quad (9)$$

where F_{TW} is the the Tracy-Widom distribution and F''_{TW} represents the second derivate of F_{TW},

$$\mu_{N,M} = \left(1 + \sqrt{\frac{M}{N}}\right)^2 \quad (10)$$

$$\sigma_{N,M} = N^{\frac{-2}{3}}\left(1 + \sqrt{\frac{M}{N}}\right)\left(1 + \frac{1}{\sqrt{\frac{M}{N}}}\right)^{1/3}. \quad (11)$$

4. Impact of the mobility

In order to motivate the necessity of improving the sensing performance in mobility, we evaluate the impact of time-varying channel on the probability density function (pdf) of the statistical test of the BCED method. First simulation result is depicted in Fig. 1 under the following parameters: $N = 10000$, $SNR = -19$ dB and $M = 5$. The pdf of the statistical test is illustrated for two different velocities (0 kmph and 350 kpmh).

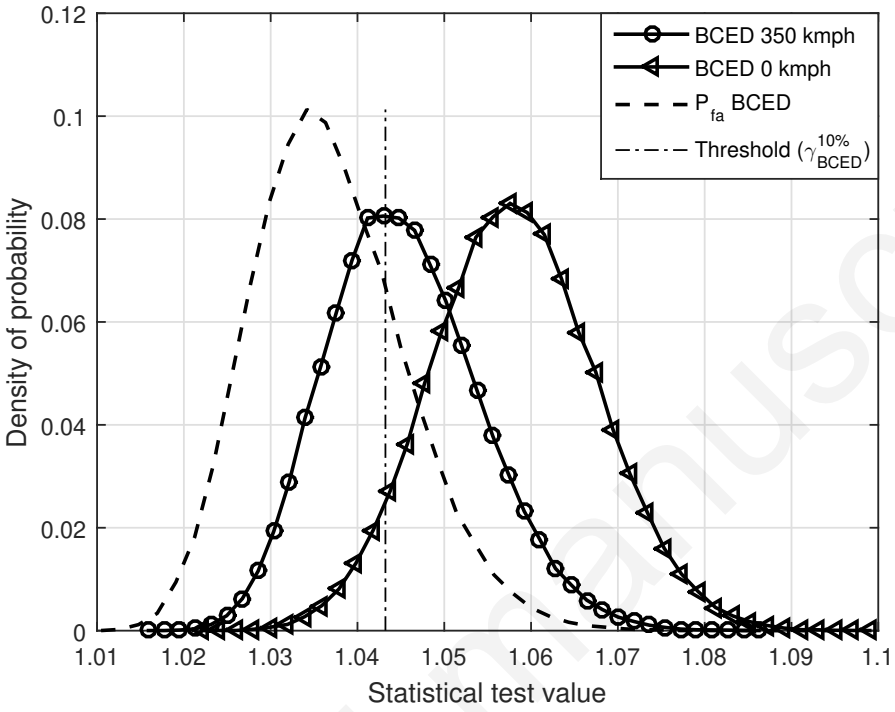

Figure 1: Impact of high mobility on the density of statistical test

In addition to the pdf of the statistical test, the dashed plot gives the pdf of false alarm and the dotted line represents the threshold and set for a probability of false alarm of 10% according to [22]. When the velocity is growing, we clearly observe that the pdf of detection is shifted towards the threshold. It is then understood that the impact of mobility is dramatic on detection performance.

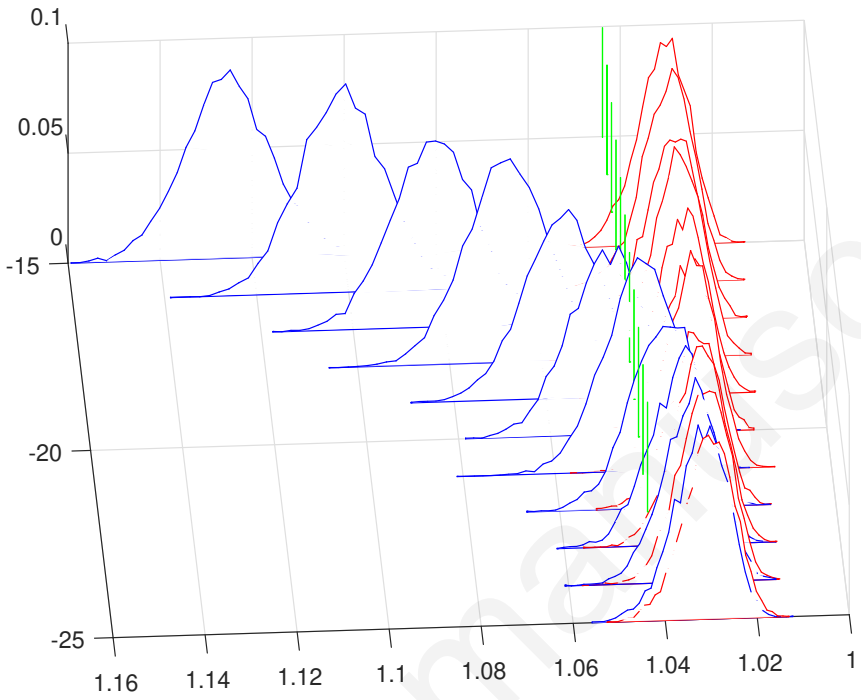

Figure 2: Probability density function of the statistical test for a velocity of 0 kmph

In Fig. 2, we evaluate the pdf of the statistical test for a velocity of 0 kmph with presence of PU (blue) and without presence of PU (red) for a SNR range of -25dB to -15dB. The green line represents the threshold fixed at 10%. We can see that the two pdf are moving away from each other from a SNR of -21dB

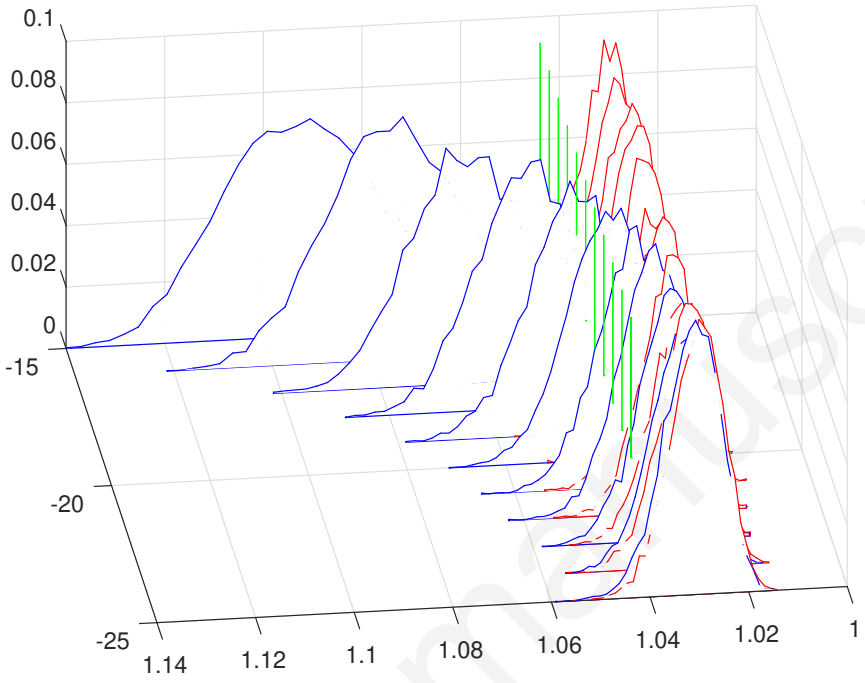

Figure 3: Probability density function of the statistical test for a velocity of 150 kmph.

In Fig. 3 and 4, we can see the impact of the mobility for different velocity 150 kmph (relative speed between two cars) and 250 kmph (train speed for railway) respectively. We can note that the two pdf (red and blue) are very close even for relatively big SNR.

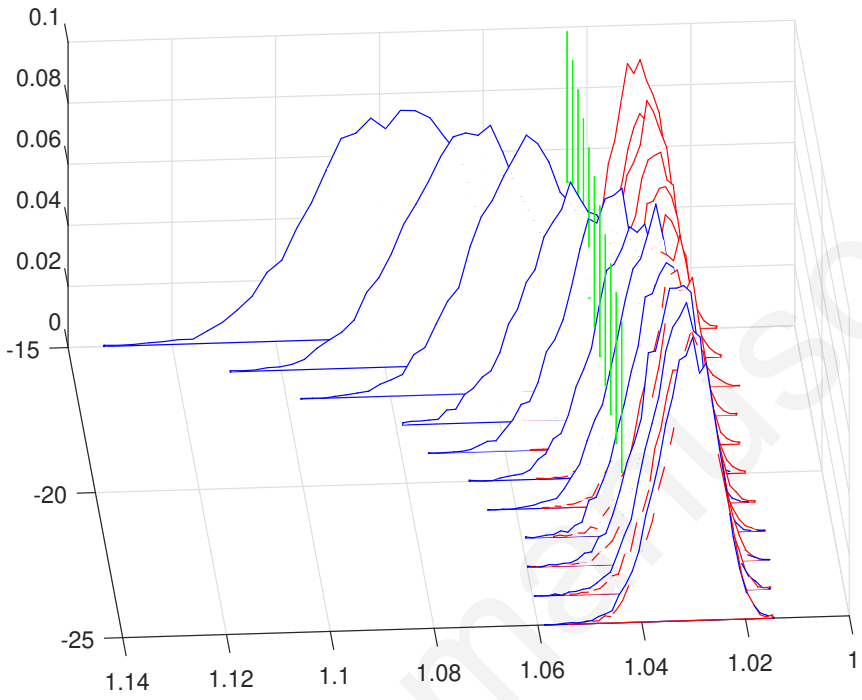

Figure 4: Probability density function of the statistical test for a velocity of 250 kmph.

In Fig. 5, we evaluate the statistical test of the BCED method (ST-BCED) under $\mathcal{H}_1$ for the different velocities ($\{0, 60, 120, 240, 360\}$ kmph) of the SU. We can see the red and the green lines corresponding to the ST-BCED under $\mathcal{H}_0$ and the threshold respectively. The parameters of simulation consider here are $N = 24000$, $M = 5$.

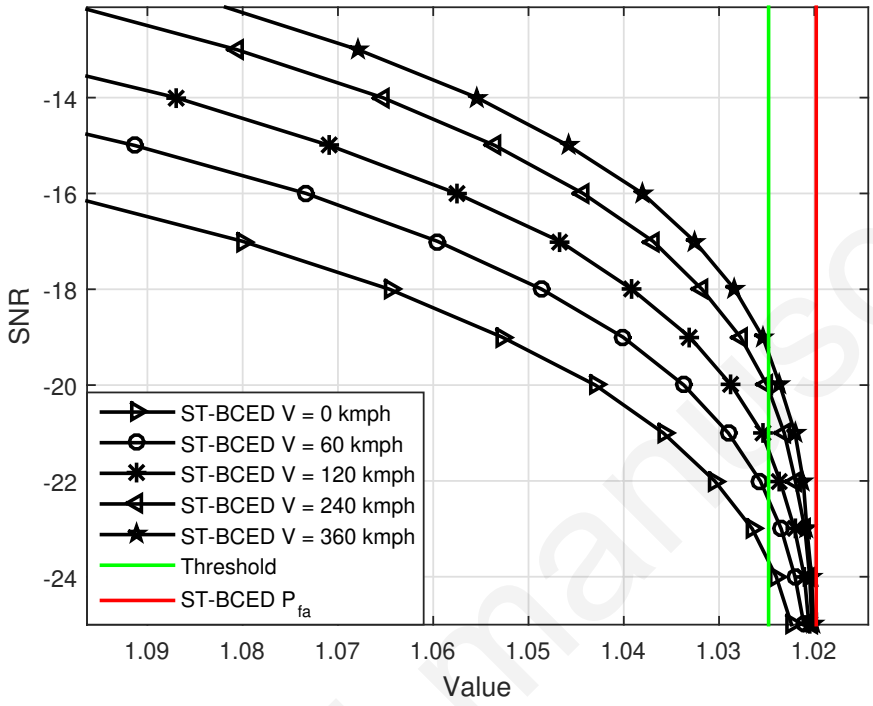

Figure 5: Probability density function of the statistical test of BCED method (ST-BCED) for different velocities.

5. Sliding window

The SW technique is widely used in the literature when facing fast time varying channels. The aim of the windowing is to attenuate the effect of the fast time-varying channels. A window is defined by considering a certain number of consecutive samples during a period which corresponds to the channel normalized coherence time $f_s T_c$, where f_s is the sampling frequency. Hence, the number of sample L_w for each window is expressed as

$$L_w = f_s T_c, \tag{12}$$

where $T_c \simeq 9/\left(16\pi f_d\right)$ is given in [23]. The number n_w of windows to consider for sliding operation is then simply given by

$$n_w = N/L_w. \tag{13}$$

In order to make reading easier, the i^{th} eigenvalue of the j^{th} window is noted $\ell_{i,j}$ in the sequel.

6. The proposed SW-BCED detection

Let us now introduce our proposal which implements the BCED algorithm along with the SW strategy. The main idea is to perform the SS at each window individually. The new statistical test can then be rewritten as follows

$$T^{j}_{\text{BCED}} = \frac{\ell_{1,j}}{\frac{1}{M}\sum_{i=1}^{M}(\ell_{i,j})}. \tag{14}$$

The statistical test at the j^{th} window is compared to the new threshold, noted $\gamma_{\text{BCED}}\{L_w\}$, considering L_w samples. Let us more investigate the denominator of (14), which corresponds to the mean energy of each window. The mean energy can be approximated by the Gaussian distribution with mean σ_b^2 and variance $\frac{2\sigma_b^4}{ML_w}$ [7]. Thus, the denominator is a deterministic variable ($ML_w >> \sigma_b^4$). Consequently, the case study can be limited to the numerator.

By assuming n_w windows, we perform the BCED algorithm in each window. In order to exploit all the results of the SS performance, if at least one window corresponding to the coherence time of the channel detects the PU, the final decision of the SU is the $\mathcal{H}_1$ hypothesis. This is equivalent to consider only the maximum value among the n_w largest eigenvalues. Hence, the statistical test becomes

$$T^{j}_{\text{SW-BCED}} = \frac{\ell_{1,j}}{\frac{1}{M}\sum_{i=1}^{M}\ell_{i,j}} \quad \text{where} \quad j = \arg\max_{k}\left(\ell_{i,k}\right) \tag{15}$$

For the sake of clarity, we denote $\hat{\ell}_{i,j}$ the estimated eigenvalues. Therefore based on the estimated values, in the practical case, we consider the highest mean energy from the n_w values. Eventually, we can restate the statistical test of the proposed SW-BCED method as follows

$$T_{\text{SW-BCED}} = \frac{\max\limits_{j}\left(\hat{\ell}_{1,j}\right)}{\max\limits_{j}\left(\frac{1}{M}\sum_{i=1}^{M}\hat{\ell}_{i,j}\right)} \underset{\mathcal{H}_1}{\overset{\mathcal{H}_0}{\lessgtr}} \gamma_{\text{BCED}}\{L_w\}, \tag{16}$$

where $\gamma_{\text{BCED}}\{L_w\}$ is the threshold of the BCED algorithm relying on L_w samples.

In order to provide more details about the work and a good overview of the proposed method, we propose the algorithm de SW_BCED and its corresponding computational complexity. The result of the comparison of the statistical $T_{\text{SW-BCED}}$ test and the threshold $\gamma_{\text{BCED}}\{L_w\}$ is a boolean expression denoted as $\mathcal{D}_{SW-BCED}$. When $\mathcal{D}_{SW-BCED}$ is true, the detector decides the presence of PU signal.

Algorithm Algorithm for SW-BCED detector

Input: N.

Output: $\mathcal{D}_{SW-BCED}$

Initialisation :

$\ell_{max} = 0$

$\text{Energy}_{max} = 0$

$L_w = 9/\left(16\pi f_D\right)$ % f_D is the normalized Doppler frequency

if $L_w > N$ **then**

  $L_w = N$

end if

Compute the threshold $\gamma_{\text{BCED}}\{L_w\}$

$n_w = N/L_w$

for $i = 0$ to $n_w - 1$ **do**

  $\mathbf{R}_y^i = \mathbf{y}\left(iL_w + 1, (i+1)L_w\right)\mathbf{y}\left(iL_w + 1, (i+1)L_w\right)^H / L_w$

  $\ell_{max}^i \leftarrow \max(\text{EVD}(\mathbf{R}_y^i))$ % EVD : Eigenvalue decomposition

  $\text{Energy}^i = \text{Tr}(\mathbf{R}_y^i)$

  if $\ell_{max}^i > \ell_{max}$ **then**

    $\ell_{max} \leftarrow \ell_{max}^i$

  end if

  if $\text{Energy}^i > \text{Energy}_{max}$ **then**

    $\text{Energy}_{max} \leftarrow \text{Energy}^i$

  end if

end for

$T_{\text{SW-BCED}} = \ell_{max}/\text{Energy}_{max}$

if $T_{\text{SW-BCED}} > \gamma_{\text{BCED}}\{L_w\}$ **then**

  $\mathcal{D}_{SW-BCED} \leftarrow$ **true**

else

  $\mathcal{D}_{SW-BCED} \leftarrow$ **false**

end if

return $\mathcal{D}_{SW-BCED}$

The complexity analysis is proposed in the following paragraph

$$\begin{aligned} \mathcal{C}_{BCED} &= \mathcal{C}_1 + \mathcal{C}_2 \\ &= \mathcal{O}\left(M \times N \times M\right) + \mathcal{O}\left(\frac{2}{3}(M)^3\right) \quad (17) \\ \mathcal{C}_{SW-BCED} &= n_w \times \mathcal{C}_{BCED} \quad (18) \end{aligned}$$

where $\mathcal{C}_1$ is the complexity of computing the covariance matrix, $\mathcal{C}_2$ is that of the eigenvalue decomposition. The sensing time depends on the number of samples, N. The value of N represents the signal duration required for spectrum sensing. The value of N is the most relevant feature for the complexity order since the value of M and n_w are very small when compared to N. Hence, the two methods are practically of the same complexity order.

7. Statistical analysis

We now aim at studying the statistical behavior of the statistical test $T_{SW-BCED}$. The numerator and denominator expressions of (16) are denoted

$$\ell_{max} = \max_j(\hat{\ell}_{1,j}) \quad (19)$$

$$\ell_{mean} = \max_j(\frac{1}{M}\sum_{i=1}^{M}\hat{\ell}_{i,j}), \quad (20)$$

respectively.

Let us first investigate ℓ_{mean} when $\xi = 0$. The mean energy can be approximated by the Gaussian distribution with mean σ_b^2 and variance $\frac{2\sigma_b^4}{ML_w}$ [7]. Thus, ℓ_{mean} is a deterministic variable and the case study is limited to ℓ_{max}.

Then, it appears that ℓ_{max} corresponds to the maximal estimated largest eigenvalue (MELE). We can then exploit the result stating that the largest re-scaled eigenvalue of the covariance matrix $\frac{\ell_{1,j}-\mu}{\upsilon}$, where

$$\mu = (\sqrt{L_w - 1} + \sqrt{M})^2 \quad (21)$$

$$\upsilon = \sqrt{\mu}(\frac{\mu}{M(L_w-1)})^{1/6}, \quad (22)$$

converges to the Tracy-Widom ($F_\beta(\gamma_{\text{BCED}})$) distribution of order β ($\beta = 1$ if the signal is real and $\beta = 2$ if the signal is complex) [22], that is,

$$\Pr\left(\frac{\ell_{1,j}-\mu}{\upsilon} < \gamma_{\text{BCED}}\{L_w\}\right) \rightarrow F_\beta\left(\gamma_{\text{BCED}}\{L_w\}\right), \quad (23)$$

where $F_\beta\left(\gamma_{\mathrm{BCED}}\{L_w\}\right)$ is the Tracy-Widom distribution of order β.

Proposition 1. *Considering n_w largest eigenvalues and L_w samples, the probability density function of the MELE, ℓ_{max} is noted $\mathcal{G}_\beta^\ell$, (see equation (32) in Appendix). In our case, $c = n_w$, $R(x)$ and $r(x)$ represent the distribution and the derivative expression of the Tracy-Widom distribution F_β respectively. The pdf expression of the MELE is finally given by*

$$\mathcal{G}_\beta^\ell = n_w F'_\beta\left(\gamma_{BCED}\{L_w\}\right) F_\beta^{n_w-1}\left(\gamma_{BCED}\{L_w\}\right), \tag{24}$$

where $F'_\beta\left(\gamma_{BCED}\{L_w\}\right)$ represents the derivate of $F_\beta\left(\gamma_{BCED}\{L_w\}\right)$.

8. Results and Discussion

Let us first validate the analytical expression in (24). In Fig. 6 we compare the pdf curves obtained through Monte-Carlo simulations (solid lines) and implementing the theoretical result of (24) (dashed lines) for $M = 5$ and $L_w = 1000$.

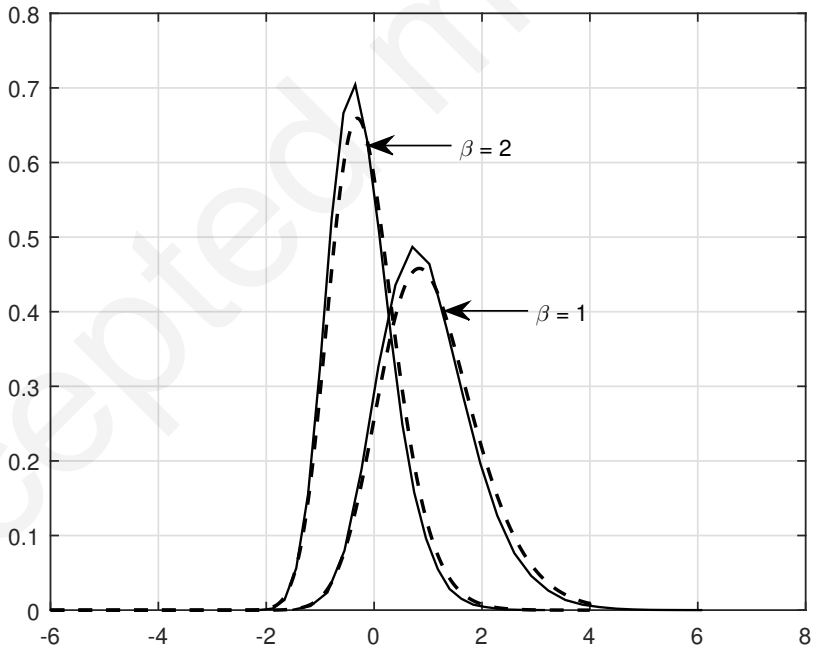

Figure 6: Probability density function of the largest re-scaled eigenvalue ℓ_{max} for $\beta = 1$ and $\beta = 2$

We can see that the theoretical values of pdf of the largest re-scaled eigenvalue and those carried out by simulations are almost the same, hence concluding that the pdf model in (24) is tight.

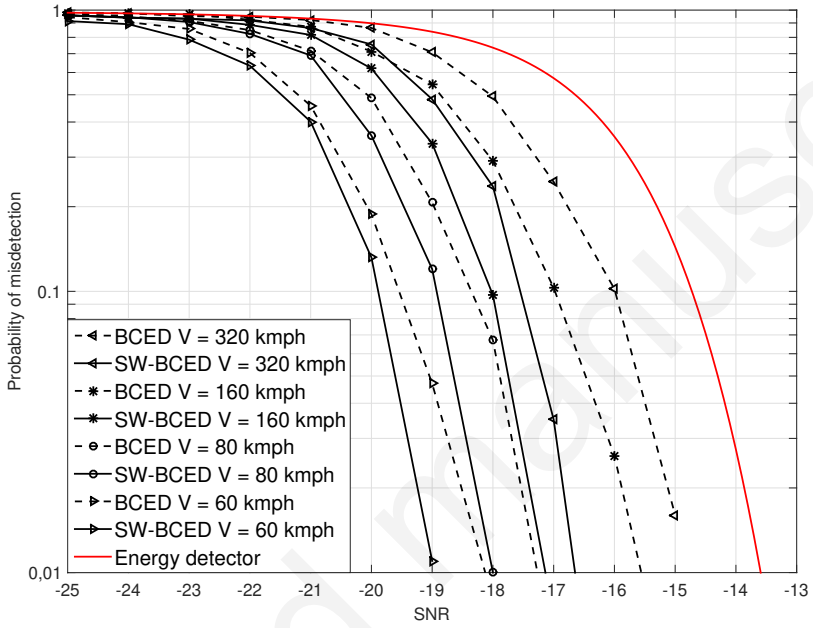

Figure 7: Probability of misdetection versus SNR for $N = 10000$ and $M = 5$

We now evaluate the proposed SW-BCED method under different parameter setting. We first compare the proposed method with the original one under different velocities and assuming a BPSK modulated signal for the PU. Fig. 7 depicts the probability of misdetection versus the SNR (dB) for different velocity $\{60, 80, 160, 320\}$ kmph and considering 1000 Monte-Carlo trials for each realization. As suggested in [23] and in order to keep a generic algorithm, we consider the normalized maximum Doppler frequency values for a carrier frequency of 2 GHz and a bandwidth of 5 MHz. It is clearly observed that the proposed SW-BCED algorithm outperforms the original one without SW whatever the velocity. But more interestingly, the SNR gain between the proposed method and the original one increases when the velocity gets higher. This proves the efficiency of the SW concept jointly used with BCED. Furthermore, we can jointly extend the sliding window

technique to other methods based on eigenvalue decomposition (see figures in "Other eigenbased methods" Appendix). Let us now compare the two methods using receiver operating characteristic (ROC) curves. The ROC curves illustrated in Fig. 8 and in Fig. 9 represent the P_d versus the P_{fa} for different numbers M of receive antennas and for different numbers N of observed samples, respectively. As expected, when the M or N increase, the detection performance improves.

However, whatever the setting, the proposed algorithm provides better performance than the original one. More precisely, on Fig. 8, the difference in terms of performance is similar for the different values of M. This can be explained by the fact that the performance gain is due to the SW size which remains constant for all M.

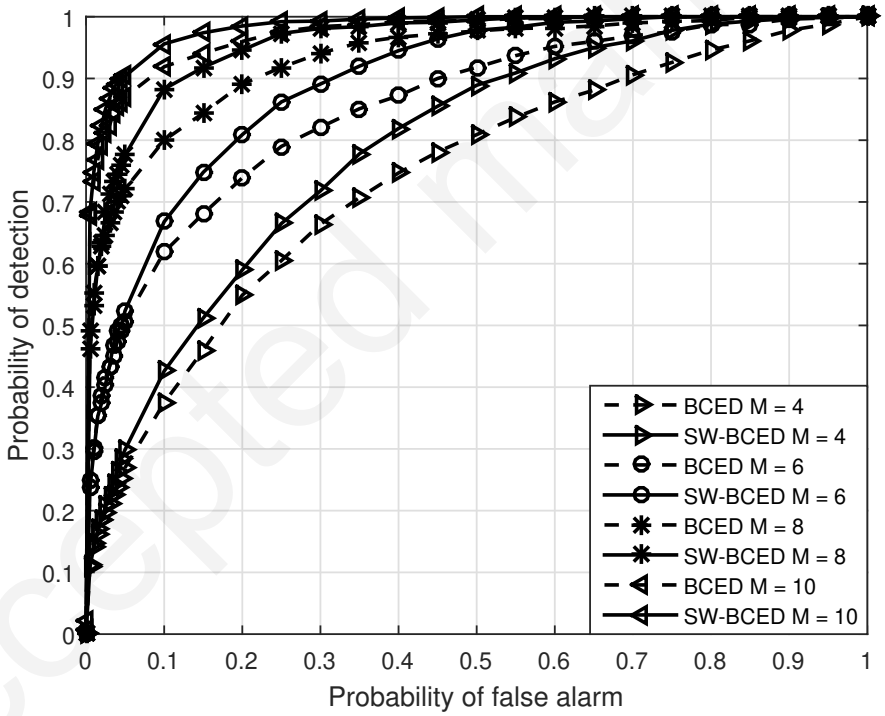

Figure 8: ROC curve for different values of receive antenna M for $N = 15000$, $SNR = -21$ dB and $v = 60$ kmph

Contrary to that, in Fig. 9, when the number N of samples increases, so does the number of windows, and the performance of the proposed SW-

BCED algorithm gets far better than the original one.

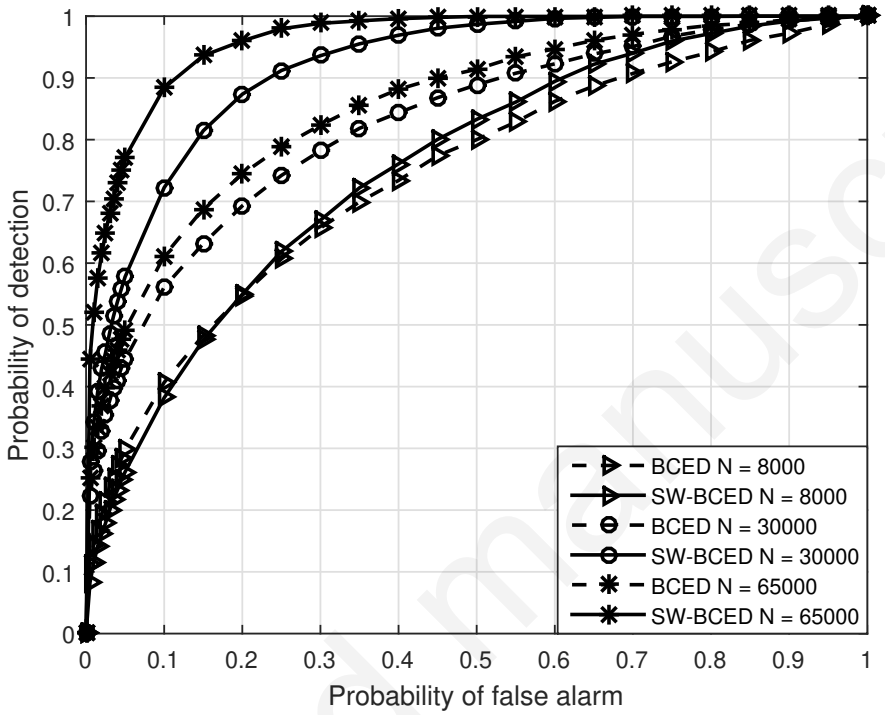

Figure 9: ROC curve for different values of receive antenna M for $M = 5$, $SNR = -21$ dB and $v = 60$ kmph

9. Conclusion

In this paper we have introduced a new blind SS method based on the EVD of the covariance matrix of the received signal combined with the sliding window concept. The aim of this method is to improve the accuracy in detecting a PU in a mobile environment. We have derived the statistical test of the proposed SW-BCED method and have provided a theoretical analysis of the MELE distribution involved in it. Through simulations, we have shown the high robustness of the proposed algorithm compared to the original one in high mobility scenarios, and whatever the number of antennas and number of observed samples.

Appendix

The probability density function of the order statistic

In this appendix, we describe the result of the order statistic of a random sample $Q_1, Q_2, \cdots, Q_d, \cdots, Q_D$. The pdf and cdf are respectively noted $r(x)$ and $R(x)$. Considering c iterations of the process, we focus our study on the pdf $r_{d,c}(x)$. First, the cdf $R_{d,c}$ is noted

$$P\left(X_{d,c} < x\right) = R_{X_{d,c}}(x) = \sum_{j=d}^{c} \binom{c}{j} \left[R(x)\right]^{j} \left[1 - R(x)\right]^{c-j}. \tag{25}$$

Hence, the number of elements in the sample less than x follows a binomial distribution $\mathcal{B}(c, j)$.

The pdf $r_{d,c}(x)$ is also given by [24]

$$\begin{aligned}
r_{d,c} =& \frac{\mathrm{d}R_{X_{d,c}}}{\mathrm{d}x} && (26)\\
=& \sum_{j=d}^{c} \binom{c}{j} \left[j \left[R(x)\right]^{j-1} r(x) \left[1 - R(x)\right]^{c-j}\right] - \Big[(c-j) \left[R(x)\right]^{j} r(x) \\
& \left[1 - R(x)\right]^{c-j-1}\Big] && (27)\\
=& \sum_{j=d}^{c} \binom{c}{j} \left[j \left[R(x)\right]^{j-1} r(x) \left[1 - R(x)\right]^{c-j}\right] - \sum_{j=d}^{c} \binom{c}{j} \Big[(c-j) \left[R(x)\right]^{j} \\
& r(x) \left[1 - R(x)\right]^{c-j-1}\Big] && (28)\\
=& \binom{c}{d} d \left[R(x)\right]^{d-1} r(x) \left[1 - R(x)\right]^{c-d} + \sum_{j=d+1}^{c} \binom{c}{j} \Big[j \left[R(x)\right]^{j-1} r(x) \\
& \left[1 - R(x)\right]^{c-j}\Big] - \sum_{j=d+1}^{c} \binom{c}{j-1} \Big[(c-j+1) \left[R(x)\right]^{j-1} r(x) \\
& \left[1 - R(x)\right]^{c-j}\Big] && (29)
\end{aligned}$$

$$= \binom{c}{d} d\left[R(x)\right]^{d-1} r(x)\left[1-R(x)\right]^{c-d} + \sum_{j=d+1}^{c} \left(\binom{c}{j} j - \binom{c}{j-1} \right.$$

$$\left. (c-j+1)) \left[\left[R(x)\right]^{j-1} r(x)\left[1-R(x)\right]^{c-j} \right] \right. \tag{30}$$

$$= \binom{c}{d} d\left[R(x)\right]^{d-1} r(x)\left[1-R(x)\right]^{c-d} \tag{31}$$

In particular for $c = d$, the pdf is given by

$$c\left[R(x)\right]^{c-1} r(x) \tag{32}$$

Other eigenbased methods

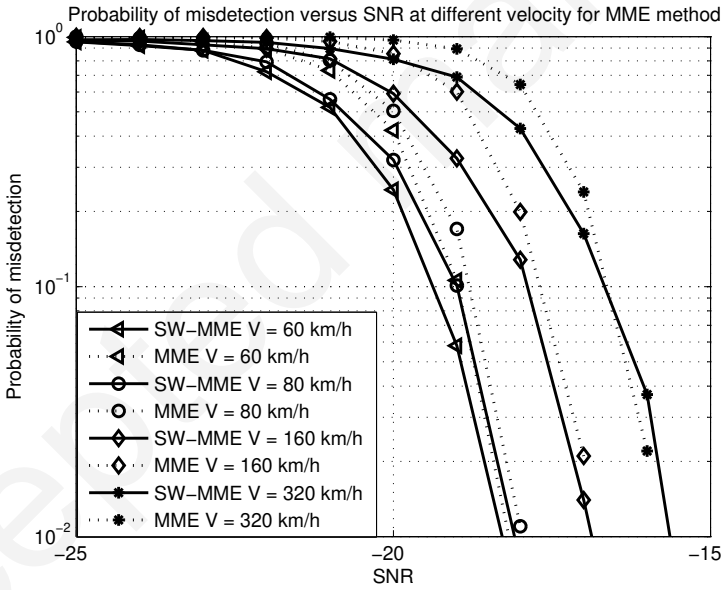

Figure 10: Probability of misdetection versus SNR at different velocity for MME method.

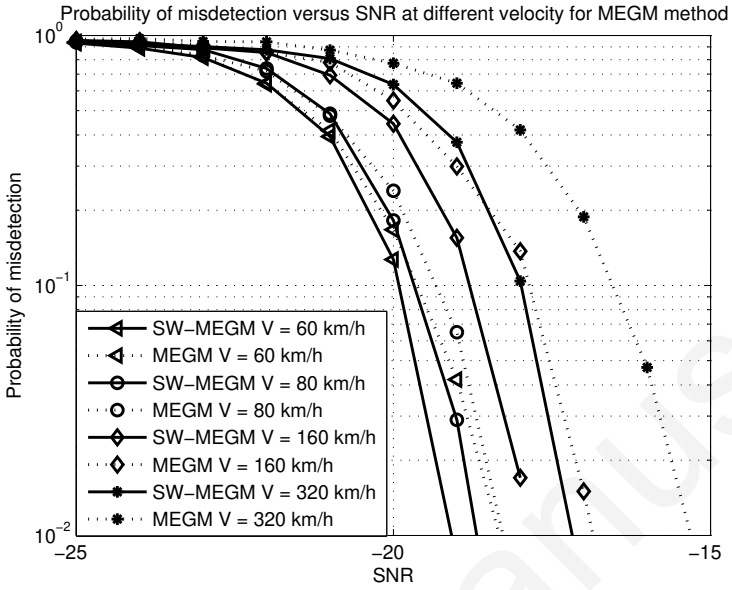

Figure 11: Probability of misdetection versus SNR at different velocity for MEGM method.

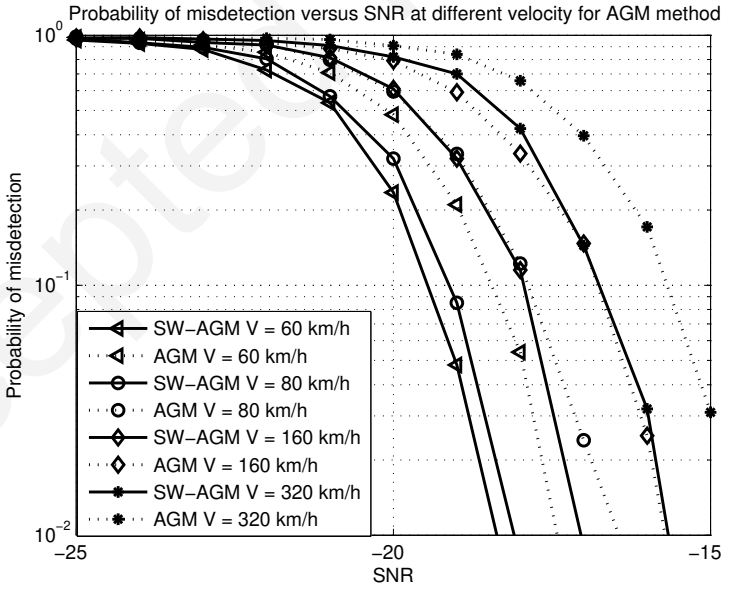

Figure 12: Probability of misdetection versus SNR at different velocity for AGM method.

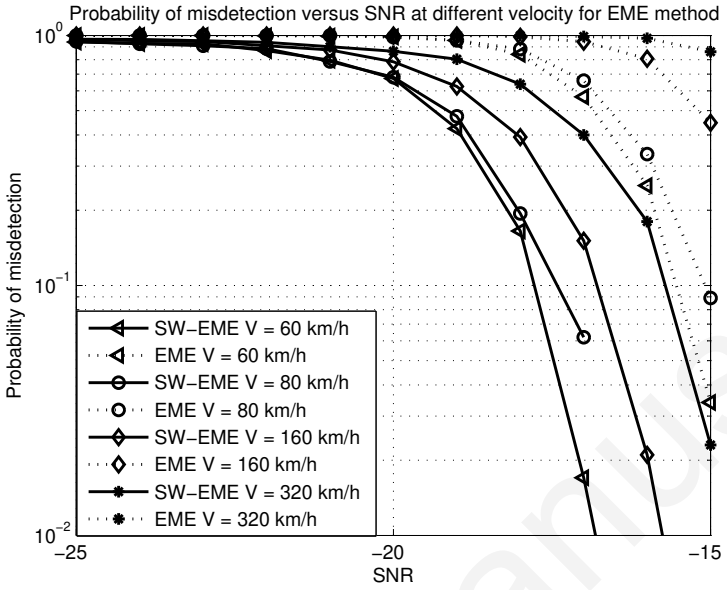

Figure 13: Probability of misdetection versus SNR at different velocity for EME method.

References

[1] K. Bouallegue, J. Baudais, M. Crussière, Unified sensing algorithm : a smart full exploitation of detection methods, in: 2019 International Conference on Wireless and Mobile Computing, Networking and Communications (WiMob), 2019, pp. 1–6. doi:10.1109/WiMOB.2019.8923570.

[2] F. A. Awin, Y. M. Alginahi, E. Abdel-Raheem, K. Tepe, Technical issues on cognitive radio-based internet of things systems: A survey, IEEE Access 7 (2019) 97887–97908.

[3] 802.22-2019 - IEEE Approved Draft Standard for Information Technology - Local and Metropolitan Area Networks - Specific Requirements - Part 22: Cognitive Radio Wireless Regional Area Networks (WRAN) Medium Access Control (MAC) and Physical Layer (PHY) Specifications: Policies and Procedures for Operation in the Bands that Allow Spectrum Sharing where the Communications Devices may Opportunistically Operate in the Spectrum of the Primary Service, IEEE Computer Society (2019).

[4] Y. Zeng, Y.-C. Liang, Spectrum-sensing algorithms for cognitive radio based on statistical covariances, IEEE Transactions on Vehicular Technology 58 (4) (2009) 1804–1815. doi:10.1109/TVT.2008.2005267.

[5] Y. Zeng, Y.-C. Liang, R. Zhang, Blindly combined energy detection for spectrum sensing in cognitive radio, IEEE Signal Processing Letters 15 (2008) 649–652. doi:10.1109/LSP.2008.2002711.

[6] R. Zhang, T. J. Lim, Y.-C. Liang, Y. Zeng, Multi-antenna based spectrum sensing for cognitive radios: A glrt approach, Communications, IEEE Transactions on 58 (1) (2010) 84–88. doi:10.1109/TCOMM.2010.01.080158.

[7] Y. Zeng, Y.-C. Liang, Eigenvalue-based spectrum sensing algorithms for cognitive radio, IEEE Transactions on Communications 57 (6) (2009) 1784–1793. doi:10.1109/TCOMM.2009.06.070402.

[8] N. Pillay, H. J. Xu, Eigenvalue-based spectrum 'hole' detection for nakagami-m fading channels with gaussian and impulse noise, IET Communications 6 (13) (2012) 2054–2064. doi:10.1049/iet-com.2011.0758.

[9] K. Bouallegue, I. Dayoub, M. Gharbi, K. Hassan, Blind spectrum sensing using extreme eigenvalues for cognitive radio networks, IEEE Communications Letters 22 (7) (2018) 1386–1389. doi:10.1109/LCOMM.2017.2776147.

[10] F. Awin, E. Abdel-Raheem, K. Tepe, Blind spectrum sensing approaches for interweaved cognitive radio system: A tutorial and short course, IEEE Communications Surveys Tutorials 21 (1) (2019) 238–259.

[11] K. Bouallegue, M. Crussière, S. Kharbech, Svm assisted primary user-detection for non-cooperative cognitive radio networks, in: IEEE ISCC 2020 - 2020 IEEE Symposium on Computers and Communications, 2020.

[12] K. Bouallegue, M. Crussière, I. Dayoub, On the impact of the covariance matrix size for spectrum sensing methods : beamforming versus eigenvalues, in: IEEE ISCC 2019 - 2019 IEEE Symposium on Computers and Communications, 2019.

[13] K. Bouallegue, I. Dayoub, M. Gharbi, K. Hassan, A cost-effective approach for spectrum sensing using beamforming,

Physical Communication 22 (Supplement C) (2017) 1 – 8. doi:https://doi.org/10.1016/j.phycom.2016.11.001.

[14] K. Bouallegue, I. Dayoub, M. Gharbi, Spectrum sensing for wireless communications using energy ratio and beamforming, in: 2017 IEEE International Conference on Communications (ICC), 2017, pp. 1–6. doi:10.1109/ICC.2017.7997142.

[15] K. Bouallegue, I. Dayoub, M. Gharbi, On low-complexity spectrum sensing: Analytical approach based spatial scanning, in: 2017 IEEE Wireless Communications and Networking Conference (WCNC), 2017, pp. 1–6. doi:10.1109/WCNC.2017.7925632.

[16] A. Chen, Z. Shi, A real-valued weighted covariance-based detection method for cognitive radio networks with correlated multiple antennas, IEEE Communications Letters 22 (11) (2018) 2290–2293. doi:10.1109/LCOMM.2018.2865346.

[17] A. Chen, Z. Shi, Z. He, A robust blind detection algorithm for cognitive radio networks with correlated multiple antennas, IEEE Communications Letters 22 (3) (2018) 570–573. doi:10.1109/LCOMM.2017.2789184.

[18] A. Paul, P. Kunarapu, A. Banerjee, S. P. Maity, Spectrum sensing in cognitive vehicular networks for uniform mobility model, IET Communications (April 2019). doi:10.1049/iet-com.2019.0128.

[19] F. A. Awin, E. Abdel-Raheem, M. Ahmadi, On the impact of acceleration on the performance of mobile cognitive radios, in: 2013 IEEE 56th International Midwest Symposium on Circuits and Systems (MWSCAS), 2013, pp. 1330–1333.

[20] T. Xu, M. Zhang, H. Hu, H. Chen, Sliced spectrum sensing—a channel condition aware sensing technique for cognitive radio networks, IEEE Transactions on Vehicular Technology 67 (11) (2018) 10815–10829. doi:10.1109/TVT.2018.2869381.

[21] W. Jakes, Microwave mobile communications, IEEE Press classic reissue, IEEE Press, 1974.

[22] B. Nadler, On the distribution of the ratio of the largest eigenvalue to the trace of a wishart matrix, Journal of Multivariate Analysis 102 (2) (2011) 363–371.

[23] S. Kharbech, I. Dayoub, M. Zwingelstein-Colin, E. P. Simon, K. Hassan, Blind digital modulation identification for time-selective mimo channels, IEEE Wireless Communications Letters 3 (4) (2014) 373–376. doi:10.1109/LWC.2014.2318041.

[24] B. Arnold, N. Balakrishnan, H. Nagaraja, A First Course in Order Statistics, Society for Industrial and Applied Mathematics, 2008. doi:10.1137/1.9780898719062.